AD-A094 760   AIR FORCE INST OF TECH WRIGHT-PATTERSON AFB OH   SCHOO--ETC   F/G 20/5
              IODINE DISSOCIATION IN A SHOCK TUBE.(U)
              DEC 80   L C FARNELL
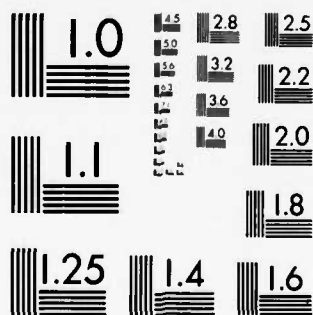UNCLASSIFIED AFIT/GAE/AA/80D-5   NL

09476

1.0
4.5
5.0
5.6
2.8
3.2
3.6
4.0
2.5
2.2
2.0

1.1

1.8

1.25 **1.4** **1.6**

MICROCOPY RESOLUTION TEST CHART
NATIONAL BUREAU OF STANDARDS-1963-A

AIR UNIVERSITY
UNITED STATES AIR FORCE

SCHOOL OF ENGINEERING

(14)

AFIT/GAE/AA/80D-5

APPROVED FOR PUBLIC RELEASE AFR 190-17.

Laurel A. Lampela
LAUREL A. LAMPELA, 2Lt, USAF
Deputy Director, Public Affairs
Air Force Institute of Technology (ATC)
Wright-Patterson AFB, OH 45433

DTIC
SELECTE
FEB 1 0 1981
D
F

(6)

(9)

IODINE DISSOCIATION
IN A SHOCK TUBE.

Master's THESIS

(10) Lawrence C. Farnell
AFIT/GAE/AA/80D-5 Captain   USAF

(11) *Dec 80*

(12) *61*

Approved for public release; distribution unlimited.

012225

81 2 09 092

IODINE DISSOCIATION

IN A SHOCK TUBE

THESIS

Presented to the Faculty of the School of Engineering

of the Air Force Institute of Technology

Air University

in Partial Fulfillment of the

Requirements for the Degree of

Master of Science

by

Lawrence C. Farnell, B.S., M.A.

Captain   USAF

Graduate Aeronautical Engineering

December 1980

Preface

This thesis is a study of infrared emissions
resulting from the dissociation of iodine in a shock tube.
It is an Air Force Institute of Technology (AFIT) project,
but much assistance has been provided by Foreign Technology
Division and Aero Propulsion Laboratory personnel at Wright-
Patterson AFB, Ohio. The Air Force is highly interested in
developing an efficient pumping mechanism for a high power
iodine laser which has many possible applications in research
and engineering. This study is an initial investigation into
the possible use of shock waves to dissociate iodine in an
electronically excited state.

My work in this field has greatly broadened my back-
ground in gas dynamics, chemical physics, chemical kinetics,
and optics. My deep appreciation goes to the Air Force and
AFIT, in particular, for this opportunity to study in such
a dynamic and professionally satisfying area. In particular,
my sincere appreciation to Dr. W. C. Elrod, who as thesis
advisor, provided me with timely direction when needed to
complete this work. My thanks to Dr. H. E. Wright and
Capt A. R. Dewispelare for their advice and support as thesis
committee members.

A special thank you to the AFIT aeronautical lab-
oratory technical staff, Mr. W. W. Baker and Mr. H. L. Cannon.
Their advice and assistance to me was invaluable. Mr. C. H.
Shortt, Mr. R. R. Ruley, Mr. J. A. Brohas, and Mr. J. G.

Tiffany, Jr. of the AFIT fabrication division provided work-
manship of exceptional quality in the timely construction of
several vital components for this project.

My most loving thank you to my wife, Cynthia, whose
sacrifice during this period is immeasurable, and to my
daughter, Leah, and son, Ryan, for providing the laughter
and diversion necessary to maintain a healthy perspective.

Lawrence C. Farnell

Contents

List of Figures

List of Tables

List of Symbols

Symbol	Description
a	speed of sound, m/sec
ΔA	vertical distance of infrared detector oscilloscope trace measured on the photograph, cm
c_f	calibration scale factor for relating infrared detector data from different tests
g	acceleration of gravity, 9.81 m/sec^2
Δh	vertical distance of test section pressure transducer oscilloscope trace measured on the photograph, cm
M	Mach number
P	gage pressure, KPa
R	universal gas constant, 8.31 joules/mole-K
Δs	distance between two pressure transducers, 1.20 m
T	temperature, K
Δt	time interval for incident shock wave to travel Δs, sec
V	velocity, m/sec
VPF	voltage-pressure factor, product of transducer sensitivity, pCb/psi, and charge amplifier setting, mv/pCb, units mv/psi
VVS	vertical-voltage setting for each oscilloscope trace, mv/cm
W	molecular weight, gm/mole
λ	wavelength, μ
γ	ratio of specific heats

<u>Subscripts</u>

1   condition in test section prior to diaphram rupture

2   condition immediately behind incident shock wave

3   condition immediately behind expansion waves

4   condition in driver section prior to diaphram rupture

5   condition immediately behind reflected shock wave

AFIT/GAE/AA/80D-5

Abstract

A two-in. (5.08 cm) I.D. circular shock tube was
assembled to study the dissociation of iodine. This study
was an initial investigation into the possible use of shock
waves to dissociate iodine in an electronically excited
state. Iodine has an emission transition in this state at
a wavelength of 1.315 µ which is used in the iodine laser.

Using argon as the diluent gas, tests were observed
with an indium-antimonide detector to determine if emissions
in the 1.1 to 5.5 µ range of the detector were present.
Tests with and without iodine were conducted at a Mach number
of approximately 2.5 with reflected shock wave temperature
of about 1570 K. Comparison of these tests indicates that a
significant infrared emission from iodine was present in the
detector range. The presence of the 1.315 µ transition can-
not yet be confirmed in that three iodine transitions exist
in the given range, other emissions from unknown sources
could be present, and the detector bandwidth could not be
suitably narrowed. Further research is required to specifi-
cally identify the spectrum of IR present.

IODINE DISSOCIATION
IN A SHOCK TUBE

I. Introduction

The scientific community is in continual pursuit of more powerful and efficient lasers. Increased power generally points to shorter operating wavelength which often leads to poorer efficiency. For this reason, the Air Force is interested in the development of an efficient pumping mechanism for a high power iodine laser. The increased power available from such a laser has many applications in research and engineering. Various pumping mechanisms have been used in attempts to increase the power available. The use of a shock wave as a pump source is investigated in this study.

Background

The quest for more powerful lasing systems has led the scientific community to search for substances which have strong stimulated emissions in shorter-and-shorter wavelengths. Recent significant interest has been given to the iodine laser with an infrared transition of wavelength $\lambda =$ 1.315 μ. Iodine photodissociation lasers operating at this wavelength have been developed. However, the search continues for an efficient pump source.

Several energy sources have been investigated as pumping mechanisms for the iodine photodissociation laser. Among the sources are multiple spark gaps, laser plasmas,

exploding wires, surface discharges, and an ultraviolet light hypocycloidal pinch device.[1] Skorobogatov[2] has suggested that since shock waves fall into the above category as powerful sources, they may be able to produce the required excitation of iodine.

It was decided that a shock tube system capable of producing strong shock waves was needed to verify Skoroboga-tov's theory. The shock tube was chosen because it is a proven, highly useful tool in the study of dissociation re-actions.[3] The central advantages of the shock tube are the controllable and predictable temperature-pressure pulse pro-duced by the shock wave, the high temperatures available, and homogeneous heating.[4] The entire region behind the shock wave is at uniform conditions, thereby, eliminating hot spots or variable temperature distributions.

A two-in. (5.08 cm) diameter, circular, constant area shock tube was obtained from the Air Force Aero Propulsion Laboratory at Wright-Patterson AFB, Ohio. This shock tube (see Section III) required complete reassembly in its new location at AFIT as well as major component reconstruction to meet the demanding requirements for iodine investigation.

Purpose and Scope

The purpose of this study was to establish a reliable technique for a thorough investigation of iodine dissociation in a shock tube. Research consisted of two distinct phases. The first was to reestablish the shock tube in a new location

2

and demonstrate its operational integrity. This required a new control system and extensive facility modification. The second phase was to use this facility to dissociate crystalline iodine in the shock tube and determine if atomic iodine in an electronically excited state could be produced. The chemical reaction could then be observed with an infrared detector to determine if the required transition emission for excited iodine was present.[5]

The essential elements of this investigation are presented in this report. Basic chemical and gas dynamic theories required for this study are given in Section II. In Section III, a detailed look at the shock tube reassembly is provided with particular emphasis on modifications required to tailor the system for this chemical investigation. The experimental apparatus and procedures are outlined in Section IV, while Section V illustrates how data was reduced. The results of this study are presented in Section VI. Finally, the conclusions and recommendations are listed in Section VII.

II. Theory

The chemical reaction and shock tube theories presented in this section and used in this study are but small highlights of more comprehensive theories of broader subjects. Chemical dissociation and the use of the shock tube in chemical investigations are treated thoroughly by a number of authors. In addition, several texts deal with complete theories of shock tube gas dynamics. The theories presented here are those portions of the broader theories which are necessary for this specific investigation. The reader is referred to the texts and papers indicated in this section for additional information.

Iodine Dissociation

When crystalline iodine (I_2) is placed in the shock tube with argon (Ar) diluent (test) gas, dissociation may be induced by a shock wave. The expected chemical reaction is postulated to be

$$Ar + I_2 \overset{K_D}{\underset{K_R}{\rightleftharpoons}} Ar + I + I \tag{1}$$
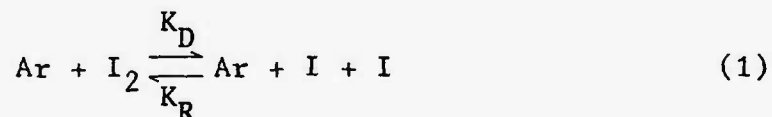
K_D is the iodine dissociation rate while K_R is the rate of reassociation.[6] Britton[7] established these rates in the range 1060-1860 K by measuring absorption at wavelength λ = 436 μ. Therefore, the degree of dissociation and dissociation rates are fairly well established.[8] Particular uncertainty exists as to the degree to which the dissociation products are

4

in the ground state or in an electronically excited state.[9]
Electronic excitation may not be significant until appreciable
or even complete dissociation occurs. Most experimenters
attempting to establish dissociation rates or concentration
generally neglect this area.

In this study, testing within the temperature range
given by Britton should assure a high degree of dissociation.
Proper selection of the test gas (diluent) can enhance the
creation of excited atoms and can influence the rate at which
the population of excited atoms decays to the ground state.[10]
Argon was selected as the test gas for this experiment
because it has been used extensively in related iodine studies
and it has a minimal effect on the depopulation of excited
iodine. Observation of the emission from iodine in the infra-
red range at $\lambda = 1.315$ μ will show that a shock wave can
produce the required excited iodine.[11]

Principles of Shock Tube Operation

The shock tube reconfigured for this study meets the
basic requirements of the previous section. It is capable of
producing a test section temperature within the required
range. It can also accommodate most test gases within a wide
range of pressures. Finally, the test section configuration
is suitable for the necessary optical observations.

This shock tube is a simple constant area device in
which a plane shock wave is produced by the sudden bursting
of a diaphram separating a high pressure gas from one at lower

5

pressure.[12] Figure 1 is a simplified diagram of the shock tube. As shown in Fig 1(a), region 1 is the low pressure section in which the test medium is placed. Region 4 is the high pressure section which contains the driver gas.

In this shock tube, diaphrams ruptured spontaneously by material failure caused by the P_4/P_1 pressure ratio. As shown in Fig 1(b), once the diaphram ruptures, a shock wave forms in the driven section while expansion waves propagate into the driver section. A contact surface separating the driver and driven gases travels into the driven section at the velocity of the gas behind the incident shock wave. Region 2 includes the part of the test gas through which the incident shock wave has passed. Region 3 contains driver gas and is that part through which expansion waves have passed.[9] As shown in Fig 1(e) and 1(f), a reflected shock wave propagates back through the test section after the incident shock wave reaches the end plate. Region 5 is the part of the driven section through which the reflected shock wave has passed.

The variation of pressure and temperature along the shock tube at a given time after diaphram rupture are illustrated by Fig 1(c) and 1(d). The initial pressure ratio is theoretically related to the Mach number of the incident
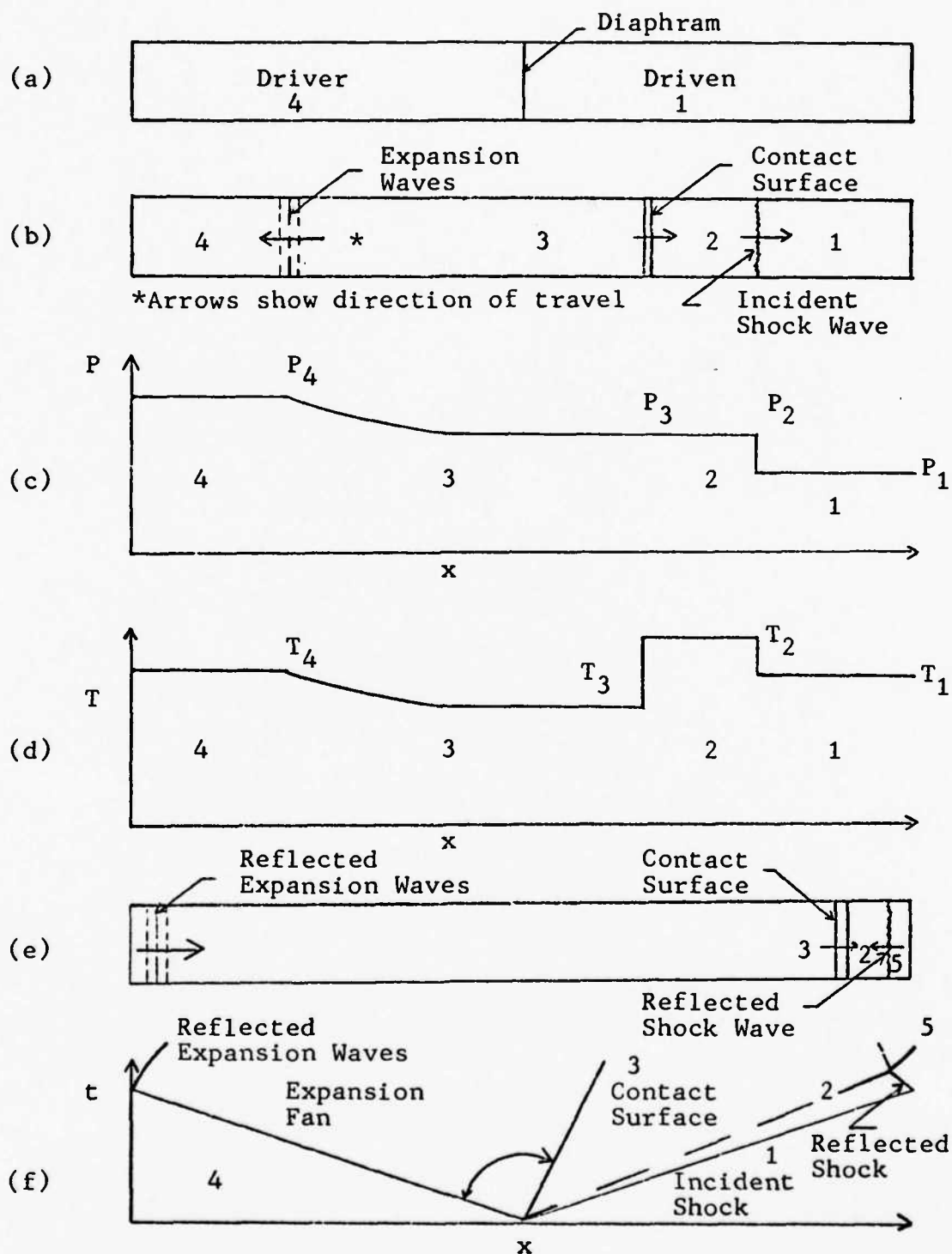
6

Fig 1. Conventional Shock Tube (a) Prior to Diaphram Rupture (b) Incident Shock Wave (c) Pressure Distribution (d) Temperature Distribution (e) Reflected Shock Wave (f) (x-t) Diagram Showing Progress of Shock Waves

7

shock wave by[9]

$$\frac{P_4}{P_1} = \left\{\frac{2\gamma_1 M^2 - (\gamma_1 - 1)}{\gamma_1 + 1}\right\} \quad \left\{1 - \frac{\gamma_4 - 1}{\gamma_1 + 1}\left(\frac{a_1}{a_4}\right)\left(M - \frac{1}{M}\right)\right\}^{\left\{\frac{-2\gamma_4}{\gamma_4 - 1}\right\}} \tag{2}$$

where P is pressure, γ is the ratio of specific heats, M is Mach number, and a is the speed of sound. Equation 2 illustrates that the pressure ratio P_4/P_1 as well as physical gas properties are important in determining shock strength.

The reflected shock wave was used in this study to further increase the pressure and temperature in the test section. Figure 1(f) is an (x-t) diagram showing the interaction of shock waves, expansion waves, and the contact surface. Theoretical relationships for pressure and temperature behind the reflected shock wave are[9]

$$\frac{P_5}{P_1} = \left\{\frac{2\gamma M^2 - (\gamma - 1)}{\gamma + 1}\right\} \quad \left\{\frac{(3\gamma - 1)M^2 - 2(\gamma - 1)}{(\gamma - 1)M^2 + 2}\right\} \tag{3}$$

$$\frac{T_5}{T_1} = \frac{[2(\gamma - 1)M^2 + (3 - \gamma)] \quad [(3\gamma - 1)M^2 - 2(\gamma - 1)]}{(\gamma + 1)^2 M^2} \tag{4}$$

where T is temperature.

Since measurements can be taken to calculate pressure and Mach number, experimental data will be used for these parameters. However, accurate temperature measurements are impractical in a shock tube. Therefore, Eq 4 will be used

8

with the actual Mach number to estimate the temperature
behind the reflected shock wave.

III. Shock Tube Assembly

General Description

The shock tube used in this study was fabricated from type 321 stainless steel tubing of modular construction and has a maximum overall length of 50 ft (15.24 m). It is a 2-in. (5.08 cm) I.D. device with 1-in. (2.54 cm) thick walls. The tube is in ten 5-ft (1.52 m) sections. This permits the experimenter to tailor driver and driven section lengths to meet the specific needs of a test. Both driver and driven sections were 15 ft (4.57 m) long for this study. The driver was moved by an electrically actuated pneumatic cylinder to provide access to the burst diaphram holder. Figure 2 is an end view of the shock tube in its current

Fig 2.   Shock Tube

10

configuration. Precise alignment of the tube in operating
configuration was accomplished both vertically and laterally
to within $\frac{1}{16}$th of an inch (.16 cm) over the entire length
with the aid of a helium-neon laser.

Diaphram Section

The double diaphram holder was capable of accommodat-
ing one or two diaphrams depending on the operating mode
selected by the operator. In the single diaphram mode, P_4
for a test run would occur at the natural rupture pressure
of the material. In the double diaphram mode, driver pressure
P_4 could be selected over a broad range above the rupture
pressure of the material. In a previous study with this shock
tube, Jones[13] provides a more detailed explanation of these
modes and diaphram materials which may be used. Jones used
this shock tube, but in a different location and configura-
tion. In addition, his study dealt with an unrelated sub-
ject. In order to get to the central issue of iodine dis-
sociation, single diaphram operation was used exclusively
for the present study.

Remote Control Operation

Possible hazards as a result of high pressure opera-
tions with toxic materials prompted construction of a remote
control operating station. This station, shown in Fig 3,
consists of two videomonitors, power supplies, pressure
reading devices, and the control panel.

11
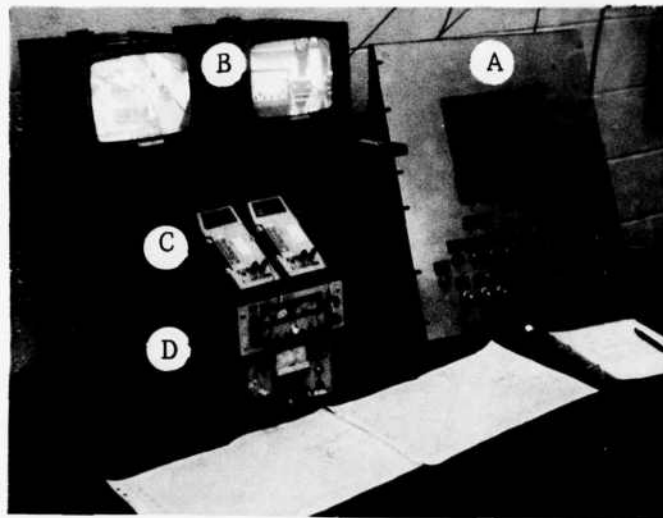
A   Control Panel

B   Videomonitors

C   Digital Voltmeters (Used to Measure Pressures)

D   Power Supplies

Fig 3.   Remote Control Operating Station

The panel is equipped with an Amphenol multipin connector which allows it to be co-located with the shock tube for system checkout. A DC power supply provides operating voltage to air control valves in the laboratory through control panel switches which, in turn, operate the high pressure pneumatic valves which control the flow of shock tube operating gases. Two commercial quality black and white television cameras were placed in the laboratory to permit remote observations.

Driver Gas Tank Farm

Shock tube location required that gas bottles be used to supply the apparatus. Though bottles can provide up to 15,000 KPa, simple series connecting of several bottles could not provide varied selection of test pressures and required bottle replacement at well above the recommended pressure. The three-bottle tank farm shown in Fig 4 was designed to permit complete depletion of gas bottles. Each bottle was individually operated from the control panel. Thirty to fifty test runs could be completed before bottle replacement was necessary.

Vacuum and Venting System

Three vacuum pumps were installed on the shock tube to establish the maximum possible vacuum prior to gas input. One pump was placed on each of the three sections; driver, double diaphram, and driven. An exhaust system for each pump

13

To Driver Gas Input
To Electrical Controls on
Remote Control Board

A   Manual Gas Bottle Valve
B   Regulator
C   Electrical Solenoid Valve
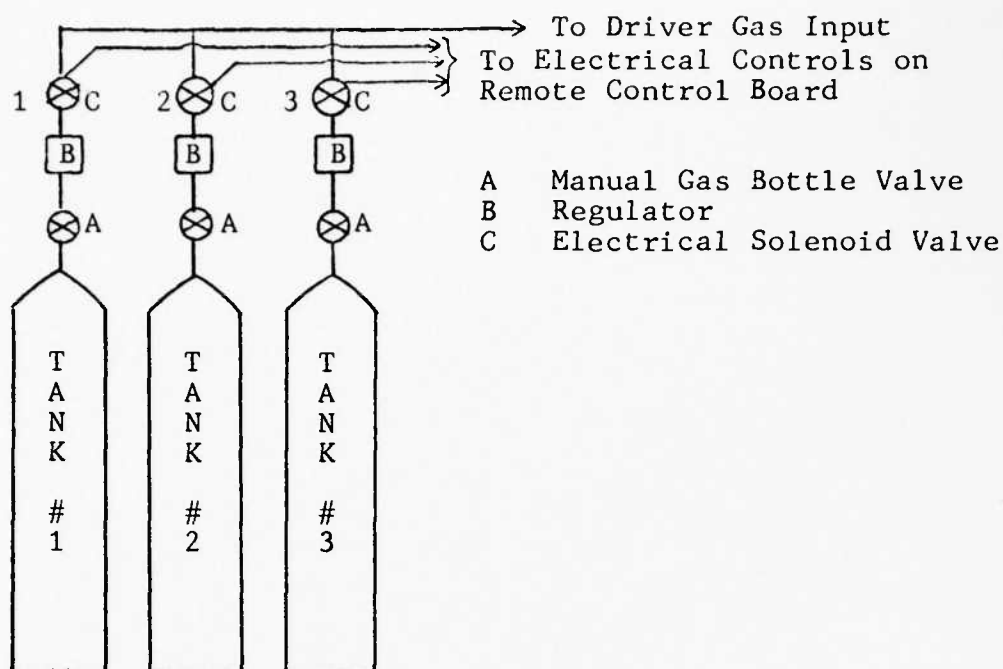
Fig 4.   Driver Gas Tank Farm

prevented accumulation of fumes in the laboratory.

Immediately following an iodine test, the shock tube
was vented through two cold traps installed in series as shown
in Fig 5. These chambers were designed to condense any iodine
remaining in the test gas onto the interior walls of the traps
before the gas was exhausted to the atmosphere. These traps
were constructed to minimize risk to personnel and the envi-
ronment posed by the inherent toxicity of iodine. Finally,
the USAF Occupational and Environmental Health Laboratory at
Brooks AFB, Texas and the Wright-Patterson AFB, Ohio Bioenvi-
ronmental Engineering Office were consulted to insure com-
pliance with federal as well as Ohio Environmental Protection
Act regulations.

14

Fig 5. Cold Traps

15

IV.   Experimental Apparatus and Procedures

Test Section

The shock tube was configured with its test section
located 15.2 cm from the end plate in the driven section of
the tube. Significant features in the test section include
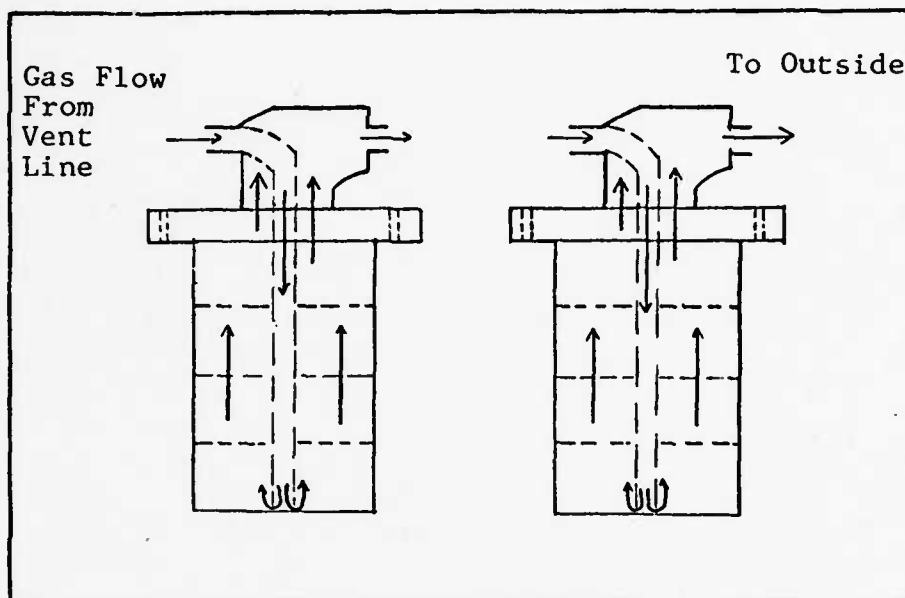an observation window and a pressure transducer. The rela-
tive locations of these items are shown in Fig 7. Infrared
emissions were observed through a 0.5-in. (1.27 cm) diameter
window. The quartz crystal pressure transducer was located
above the window. A particle injector was located just up-
stream of the window.

Particle Injector. An aerodynamic shape in the form
of a flat plate with sharpened wedge-shaped leading and
trailing edges was soldered into a thin-wall stainless steel
tube at zero angle of attack to support crystalline iodine
test samples and function as the particle injector for this
study. The injector, as shown in Fig 6, was 11.4 cm upstream
of the test section window.

At the start of each test, an iodine sample was
placed on the injector and the tube was inserted into the
test section. After the injector was aligned within the test
section, the end plate was secured.
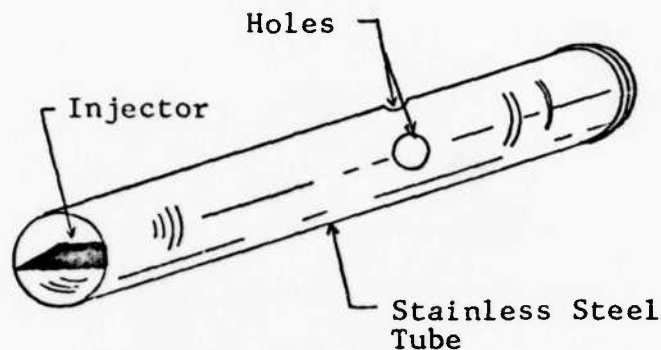
Fig 6.   Particle Injector

Figure 7 illustrates both the sequence of events and the physical layout of the test section during a test.   As the shock wave passed over the injector, it was postulated that the particles would be dispersed throughout the test section as shown.   Behind the reflected shock wave a near uniform field of stationary iodine particles would dissociate if the reflected shock wave was of sufficient strength.   This dissociation could then be observed through the test section window.

Instrumentation.   Test instrumentation includes static and dynamic pressure measuring devices and an infra-red detector.   Driven section static pressure, P_1, was measured before each test with a Heise 0-30 psig (0-200 KPa) gage.   Driver section static pressure, P_4, and double diaphram

17
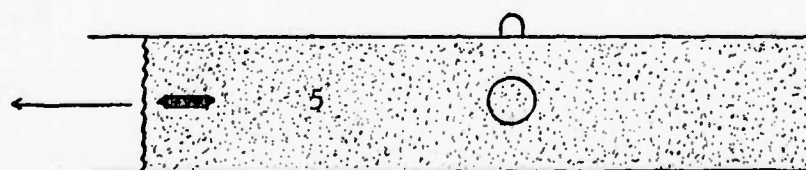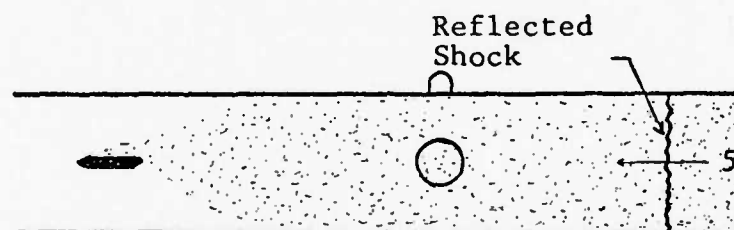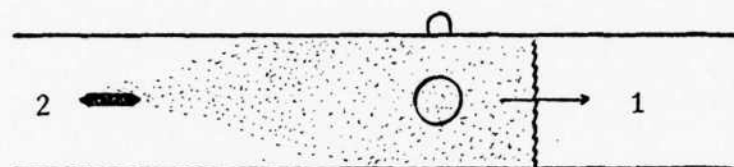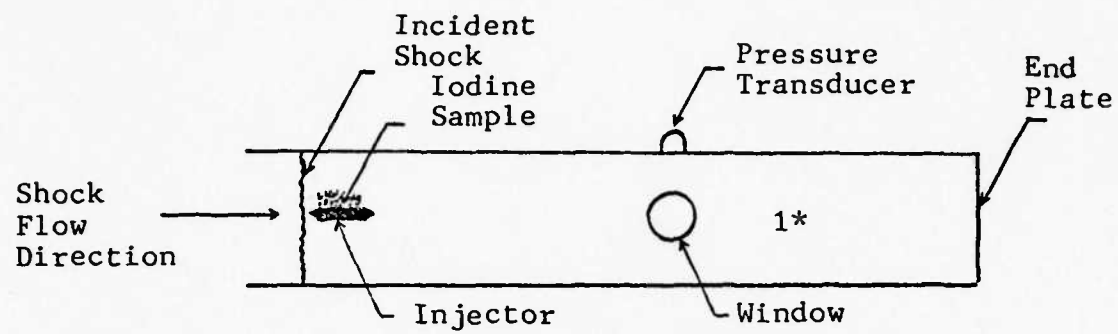
*See Fig 1 for Region Identification

Fig 7. Sequence of Events in Test Section

18

section pressure, were measured locally with two Ashcroft 0-3000 psig (0-20,700 KPa) gages and remotely with two Viatran model 104, 0-2000 psig (0-13,800 KPa) pressure transducers with readout on digital voltmeters. Dynamic pressure measurements were made with two Kistler model 603A quartz crystal pressure transducers. One transducer was located 120 cm upstream from the test section window, while the other was located above the window as noted in Fig 7. These transducers were used to calculate shock speed and reflected shock pressure, P_5 (see Section V). The optical system was used to detect the presence of infrared emissions through the window. These items are listed in Table I as instrumentation and are illustrated in Fig 9.

Optical System. The optical system, shown in Fig 8, included a calcium floride lens, a silicon filter, pinhole, and a liquid nitrogen cooled indium-antimonide detector.[14] The lens was used to focus emissions from the test section onto the detector. The filter blocked all emissions shorter than 1.1 μ. The pinhole was mounted directly in front of the detector. The Barns Engineering detector has an operating range of 1.0 to 5.5 μ and a 1 μsec response time at 77 K. The detector was mounted on a three-degree-of-freedom translating mount to permit precise alignment.

Support Equipment. Items necessary to operate the shock tube and collect test data are included in Table I as

19
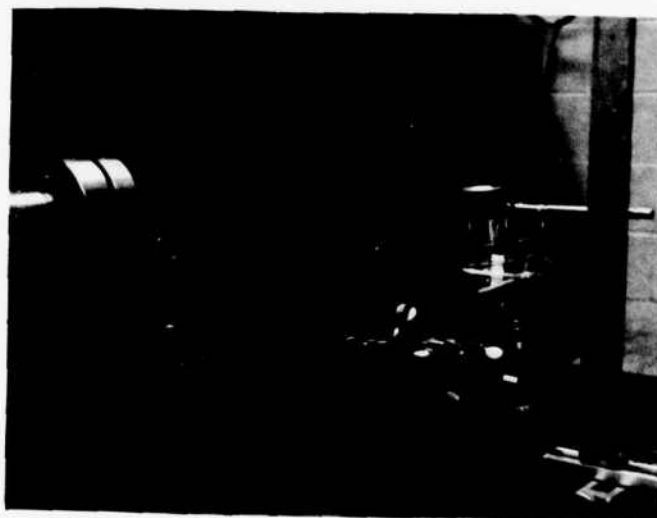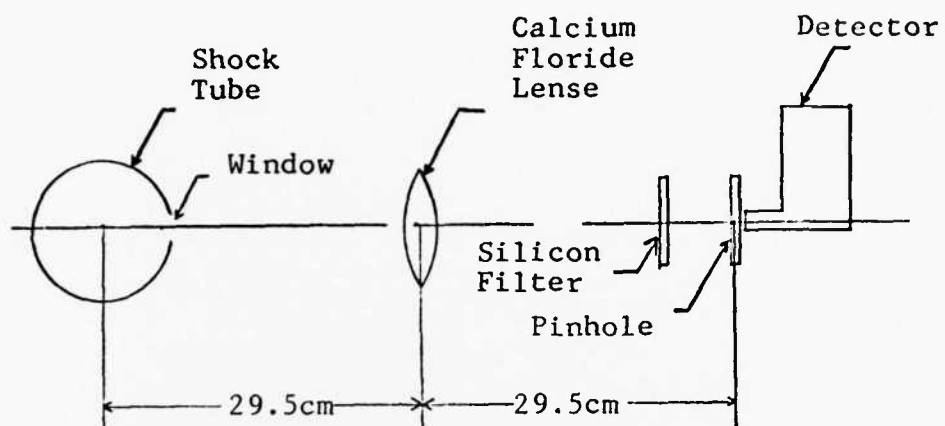
Fig 8.   Optical System

support equipment. The function and sequence of action of
specific items during a test are presented in Table I and
Fig 9. Elaboration on these items is given below and in
other sections of the text.

Test time was on the order of 100 msec as measured
from diaphram rupture until the reflected shock wave was
well out of the test section. Instrumentation and support
equipment operation during each test began with incident
shock wave arrival at the upstream pressure transducer. An
electrical output signal caused by the pressure pulse from
the shock wave on the crystal transducer was sent to a charge
amplifier. After amplifying the transducer signal, the
charge amplifier output signal was sent to the triggering
mechanism of the type 551 Tektronic oscilloscope. The
oscilloscope triggering system then started the Beckman
electronic counter. In a similar manner, the counter was
stopped through the type 535 Tektronic oscilloscope trigger-
ing mechanism upon incident shock arrival at the test section
pressure transducer. The infrared detector was operated con-
tinuously during each test. Output signals from both the
detector and the test section pressure transducer were momen-
tarily written onto both oscilloscope CRTs and photographic
film. Oscilloscope sweep rates were controlled to insure
output signals could be recorded for several milliseconds
after reflected shock arrival in the test section. The
support equipment was reset prior to the next test.

TABLE I

Instrumentation and Support Equipment

Item	Function
Instrumentation	
1. Quartz crystal pressure transducer, Kistler 603A, (2)*	Triggered oscilloscopes and measured P_2 and P_5
2. Gage, Heise 0-30 psig (0-200 KPa)	Measured P_1 before test
3. Gage, Ashcroft 0-3000 psig (0-20,700 KPa) (2)	Measured P_4 and double-diaphram section pressure before test (locally)
4. Static pressure transducer, Viatran model 104 (2)	Same as 3, but remotely
5. Infrared detector, Barnes Engineering indium-antimonide	Measured infrared output of test medium
Support Equipment	
6. Charge Amplifier, Kistler model 566, (2)	Signal amplifier from transducer to scope
7. Oscilloscope, Tektronic type 551	Displayed pressure and infrared output and started counter
8. Oscilloscope, Tektronic type 535A	Displayed pressure and infrared output and stopped counter
9. Electronic counter, Beckman model 7360	Measured incident shock travel time
10. Camera, Tektronic C-12 (2)	Recorded oscilloscope traces

22

TABLE I (Continued)

11.	Gage, US Gage 30(VAC)-60 in-Hg gage (3)	Measured effective vacuum in shock tube
12.	Vacuum Pumps (3)	Evacuated shock tube
13.	Power Supply, Hewlett-Packard, model 6205B	Provided input power for 4 above
14.	Multimeter, Fluke model 8022A (2)	P_4 and double diaphram section pressure readout
15.	Power Supply, Trygon Electronics, model HR20-15	Provided DC control power for shock tube
16.	Calibrator, Kistler model 541A	Calibrated transducer, charge amplifier, scope triggering circuits
17.	Lense, Calcium Floride	Focused infrared emission from shock tube
18.	Filter, Silicon	Cut out all emissions into detector shorter than 1.1 μ
19.	Pinhole	Focusing point of lense
20.	Battery, Eveready model BA-230/u, 10 1/2 VDC	Input power to preamplifier
21.	Preamplifier, Perry Associates, model 720	Amplified detector output signal
22.	Alignment coil, 1 mm diameter nichrome wire	Infrared radiation source to align detector
23.	Television Camera, Phillips model LDH 0051/07 (2)	Remote observation of laboratory
24.	Television Receivers, Panasonic, model TN-93 (2)	Same as 23

TABLE I (Continued)

25.	Electronic Scale Balance, Mettler Instrument Corporation, model B6	Weighed iodine test samples

*Indicates quantity of item needed

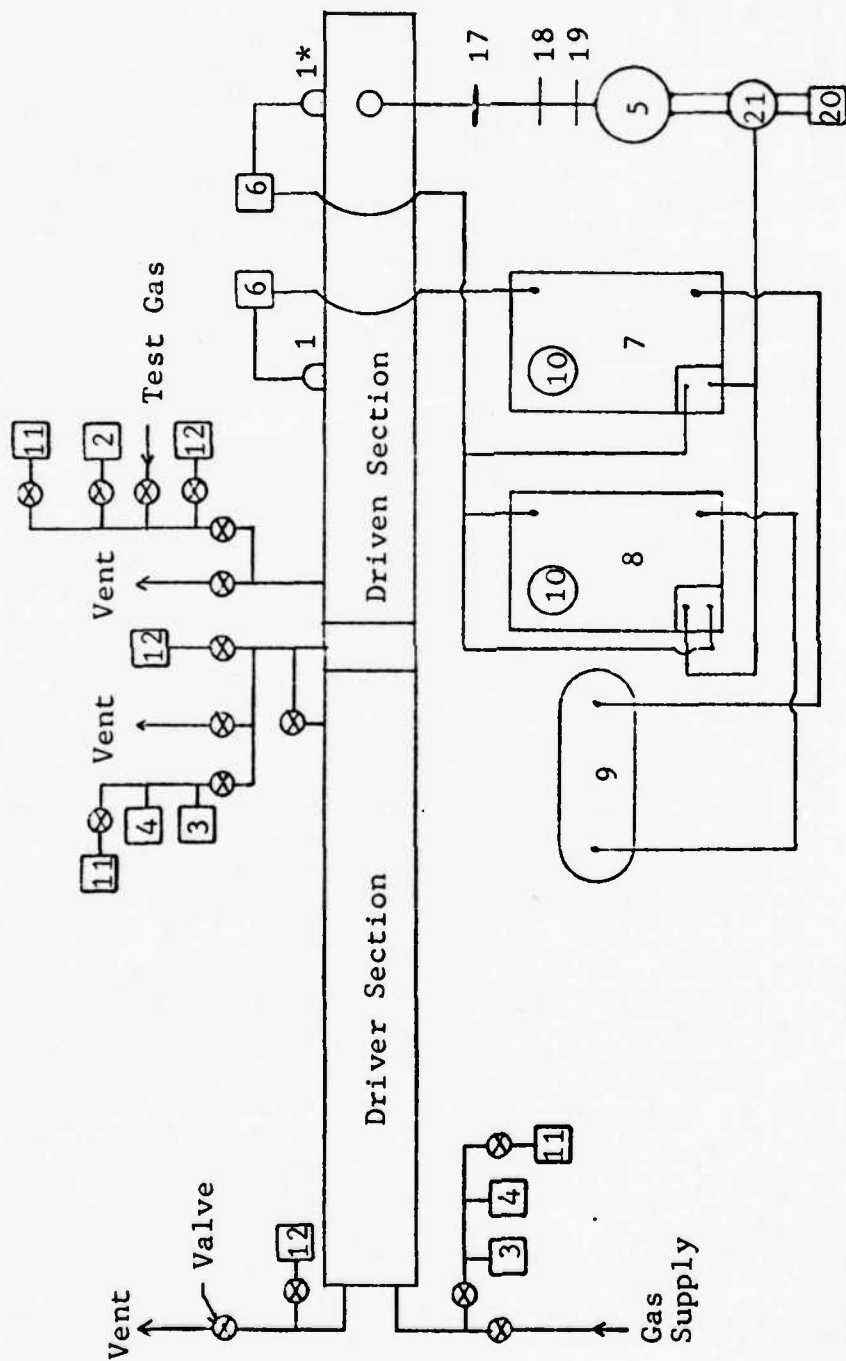Fig 9. Instrumentation and Selected Support Equipment

*Numbers Refer to Table I

25

Operating Procedures

Shock tube operating procedures required precise
calibration and alignment of test equipment and specific
test procedures to verify the accuracy of test data and
insure test repeatability.

Instrumentation Calibration and Alignment. The
Viatran and Kistler pressure transducers were calibrated
in accordance with standard practice and manufacturer's
specifications. Voltage output from the Viatran transducers
was plotted against pressure to measure P_4 over the required
range for each test. Kistler transducer sensitivity (slope
of calibration curve) was established so that P_5 could be
accurately calculated (see Section V). Once the test and
support equipment were fully assembled, the Kistler cali-
brator was used to balance charge amplifier voltage output
with oscilloscope triggering sensitivity and starting and
stopping of the counter.

The infrared detector was operated with zero bias
voltage on the detector element. Calibration and alignment
of the detector was performed by inserting a nichrome wire
heating coil inside the shock tube at the test section
window.[14] The light source was focused on the pinhole.
A mechanical chopper placed to interrupt the light beam
produced a square wave signal output from the detector on
the oscilloscope. The detector was then aligned with the

26

translating mount to maximize the amplitude of the square
wave signal.

Shock Tube Operation. Operating checklists were
prepared to simplify and standardize each test. At the
beginning of each day, the infrared detector dewar was
filled with liquid nitrogen to cool it to an operating
temperature of 77 K. Care was taken to remove all moisture
from the dewar to prevent ice formation which could damage
the unit. Once the detector was cooled, the preamplifier
was turned on and the detector was aligned.

Each cold trap, Fig 5, was immersed in a dry ice-
isopropyl alcohol bath to cool it to approximately 195 K.
The baths were checked periodically for proper operation.

The driver section and knife edge were cleaned prior
to each iodine test with acetone, a ramrod device, and a
high pressure compressed air hose. The test sample was then
placed on the knife edge and the injector was inserted into
the test section. The transducer and end plate were secured
before the diaphram was inserted and the diaphram section
sealed. The shock tube was then evacuated to less than
0.13 KPa before the driver section was filled to 104.43 KPa
with argon test gas. Test and support equipment were re-
checked to insure oscilloscope single sweep operation was
set, traces were properly aligned on the graticule, trig-
gering sensitivity was set, camera shutters opened, and
counter reset. Helium was introduced into the driver section

27

through the tank farm until the diaphram ruptured. The
shock tube was then vented through the driven section vent
line and cold traps. Before opening the shock tube, it
was evacuated through the cold traps with the driven section
vacuum pump. The camera film was developed and the tube
prepared for another test.

Test Samples. Test samples were obtained from
polycrystalline iodine meeting American Chemical Society
specifications which assayed at 99.8% pure. Major contam-
inates were 0.010% nonvolatile matter and 0.003% chlorine.
Samples were finely ground in a mortar with a pestle in a
vented laboratory prior to weighing on an electronic balance
(see Table I). Each sample, weighing 200 mg, was placed in
a sealed glass bottle until needed for testing.

V. Data Reduction

Experimental data was used to calculate shock velocity, reflected shock pressure, and infrared emission intensity. Theoretical methods were used to determine reflected shock temperature as outlined in Section II. Data for some runs are included in the appendix.

Incident Shock Wave Velocity

The velocity of the incident shock wave was determined by measuring the time Δt between shock arrival at the upstream and test section pressure transducers with an electronic counter. In Fig 10, an oscilloscope trace of a typical argon gas and iodine test shows the test section pressure transducer on the upper trace and the infrared detector on the lower trace. The accompanying diagram identifies measurements necessary for data reduction. Shock wave velocity V was determined by

$$V = \frac{\Delta s}{\Delta t} \tag{5}$$
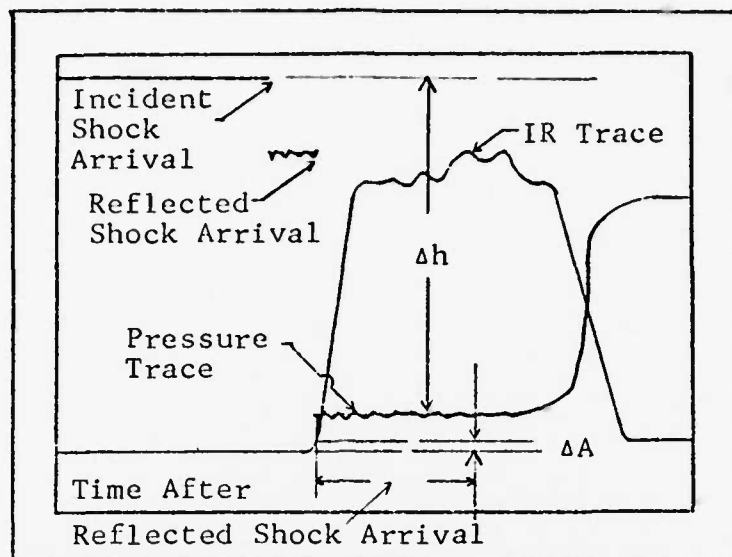
where $\Delta s = 120$ cm. Shock Mach number M was calculated using

$$M = \frac{V}{a_1} \tag{6}$$

where the speed of sound in the test gas,

$$a_1 = \sqrt{\gamma \frac{R}{W} T_1} \tag{7}$$

was calculated for each run.

29

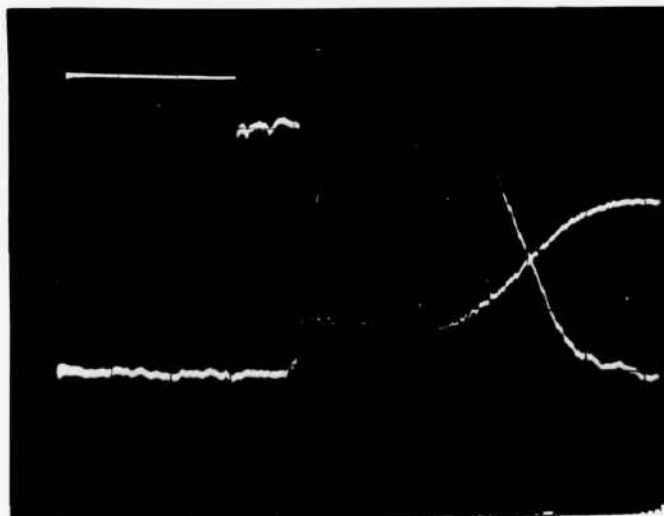Run Number 28S2   VVS = 10 mv/cm

Fig 10.   Photograph of CRT Output of Test
          With Iodine Using the Plexiglass
          Window

Reflected Shock Pressure

The pressure behind the reflected shock wave P_5 was calculated for each run from oscilloscope photographs similar to Fig 10. The trace distinctly shows both incident and reflected shock arrival in the test section. After Δh was measured, the reflected shock pressure was calculated by

$$P_5 = P_1 + \frac{\Delta h(VVS)}{VPF} \tag{8}$$

VVS is the vertical voltage range scale setting and VPF is the voltage pressure factor. VPF is the product of transducer sensitivity and charge amplifier setting.

Infrared Emission

Detector output voltage was calculated by multiplying the detector trace amplitude ΔA by VVS (see Fig 10). Voltage was determined for each run at 0.5 msec intervals for 2.5 msec after reflected shock arrival. This data was used to compare those runs with iodine to those without iodine.

Reflected Shock Temperature

Reflected shock temperature was determined from Eq 4 using $\gamma = 1.667$ and M.[9] Careful consideration was given to including real gas effects and variable γ.[15] In that the argon test gas was monatomic and moderate temperatures were used, assuming a constant γ had a negligible impact on temperature calculations.[9]

31

VI. Results and Discussion

Since the shock tube facility was reestablished in
a new location, 35 initial test runs were made without iodine
to demonstrate repeatability and verify reliability of the
system. These tests were conducted to establish the opera-
tional integrity of the shock tube in fulfillment of the
first major objective of this study. The effort was then
turned to the iodine problem.

Forty-three additional runs were conducted in sup-
port of the iodine dissociation objective. Nineteen of these
tests were with iodine. Iodine runs began at $P_4/P_1 = 12.5$.
Driver section pressure P_4 was steadily increased on subse-
quent runs until a strong infrared signal was obtained.

Argon was chosen as the test gas because it has been
used extensively in similar studies.[6, 7, 10, 15] Helium was
also used in the same P_4/P_1 range. Due to the difference in
molecular weight, T_5 and M were too low to obtain an infrared
emission. Rather than conduct helium-iodine tests at higher
pressures, it was decided to limit this study to argon and
leave helium for a later effort.

Argon has two emission wavelengths in the range of
the detector.[5] These were observed during tests without
iodine. However, the detector responds to all emissions
within its operating range. In the scavenging of the system
by high vacuum, some residual gas in the tube walls and
chamber volume could not be eliminated. Since contaminates

32

were present in the same quantities in all tests, the emission characteristics due to argon and possible contaminates should be approximately the same.

Four tests were selected for data presentation. Three of these were without iodine while one included iodine. These four tests were selected based on nearly identical P_4/P_1, P_5/P_1, M, and T_5. In addition, photographic quality and diaphram petalling characteristics were judged approximately the same for these runs. A summary of experimental data is presented in the appendix. The ranges of selected parameters for these runs is given in Table II.

TABLE II

Range of Selected Parameters

Parameter	Range	Percent Difference
P_4/P_1	33.4 – 34.4	2.9
P_5/P_1	36.2 – 38.4	6.1
M	2.52 – 2.59	2.8
T_5	1564 – 1594 K	1.9

A plexiglass test section window was used for the one iodine test and one test without iodine before the quartz window was installed. A quartz window was later obtained and was used for the two remaining runs. Figure 10 (Section V) is the iodine test while Fig 11 is the test without iodine,

33

Run Number 30S1   VVS = 10 mv/cm
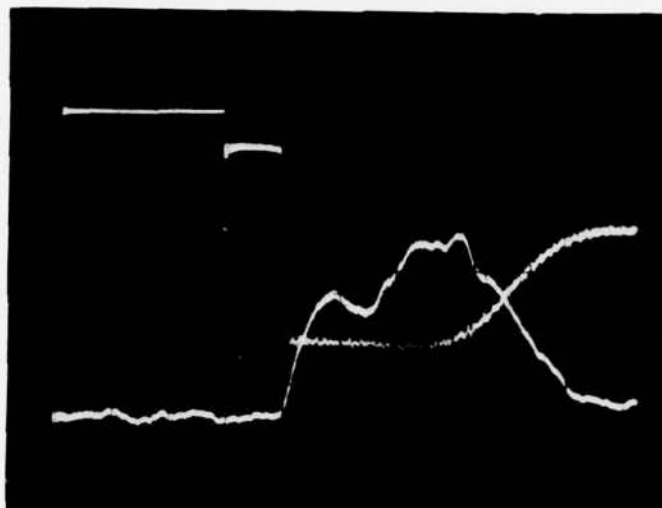

Fig 11.   Photograph of CRT Output of Test
          Without Iodine Using the Plexi-
          glass Window

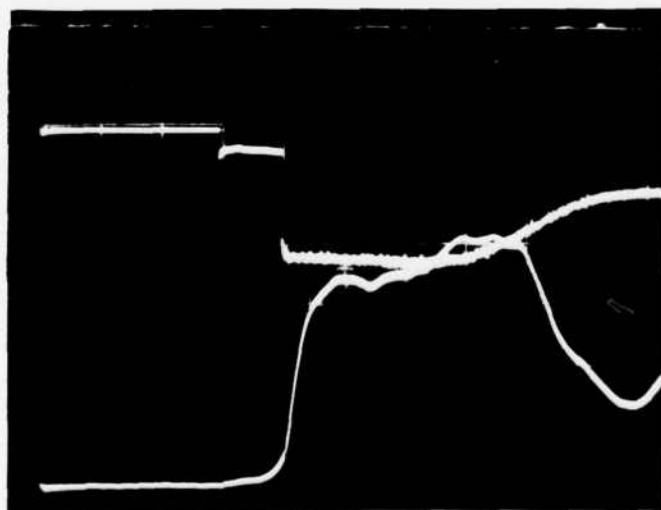Run Number 603   VVS = 50 mv/cm

Fig 12.   Photograph of CRT Output of Test
          Without Iodine Using the Quartz
          Window

both using the plexiglass window. One of the runs without iodine using the quartz window is shown in Fig 12. Though the detector output traces in Figs 11 and 12 appear similar, notice that there are some differences in their vertical deflections.

It is clear from these photographs that the plexiglass window distorted the infrared emissions during the tests. Since the detector output voltage is a measure of the overall intensity of the infrared emissions over the 1.1 to 5.5 μ range, the plexiglass runs can be related to the quartz runs by a calibration scale factor, c_f.

The scale factor is based on the detector calibration photographs in Fig 13. Figure 13(a) was obtained by aligning the detector to its maximum possible amplitude using the nichrome wire alignment coil (see Section IV) and the quartz window. Figure 13(b) was obtained by replacing the quartz window with the plexiglass window and adjusting the vertical voltage setting on the oscilloscope. The calibration scale factor is

$$c_f = \frac{(\Delta A) \ (VVS) \ \text{Quartz}}{(\Delta A) \ (VVS) \ \text{Plexiglass}}$$

$$= \frac{(4.5 \text{ cm}) \ (200 \text{ mv/cm})}{(2.9 \text{ cm}) \ (\ 50 \text{ mv/cm})}$$

$$c_f = 6.2 \quad \quad . \quad \quad \quad (9)$$

Infrared trace data from Figs 10 and 11 was multiplied by c_f to relate the runs with the plexiglass window to the runs with the quartz window. Figure 14 shows detector

35

(a)
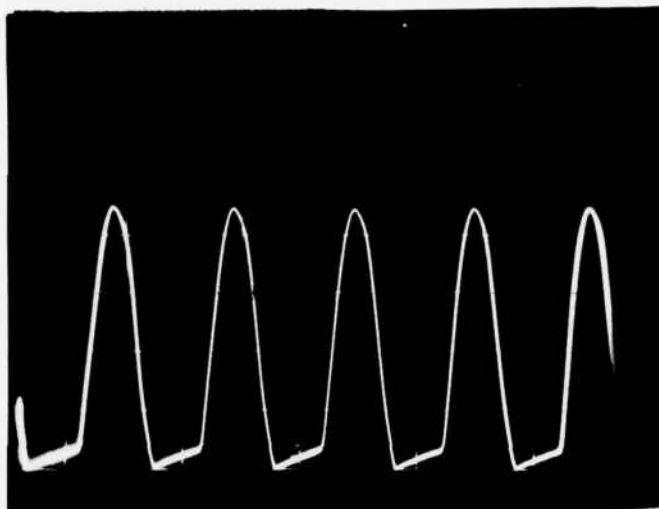
ΔA = 4.45 cm   VVS = 200 mv/cm

ΔA = 2.9 cm   VVS = 50 mv/cm

(b)
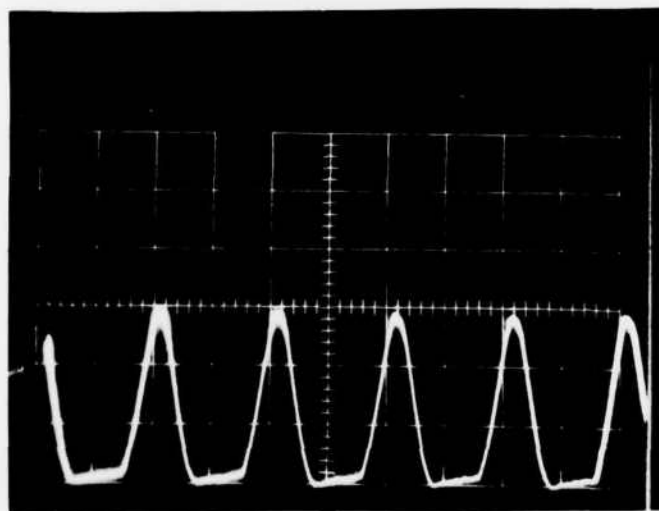
Fig 13.   Photographs of CRT Output of
          Calibration Light Source, (a)
          Quartz Window, (b) Plexiglass
          Window

36

output voltage over time after reflected shock arrival for the three tests without iodine. The test with the c_f adjusted data falls directly between the two runs that used the quartz window. This result lends definite validity to the calibration scale factor adjustment technique for this application.

The three runs from Fig 14 were averaged and are given in Fig 15 as the "without iodine" curve. The c_f adjusted data from Fig 10 is the "with iodine" curve in Fig 15. This comparison indicates that a significant infrared emission in the $1.1 - 5.5$ μ range is present due to the iodine.

Fig 14. Infrared Detector Output After Reflected
Shock Arrival in Test Section For Runs
Without Iodine

Fig 15.   Infrared Detector Output After Reflected
          Shock Arrival in Test Section For Runs
          With and Without Iodine

39

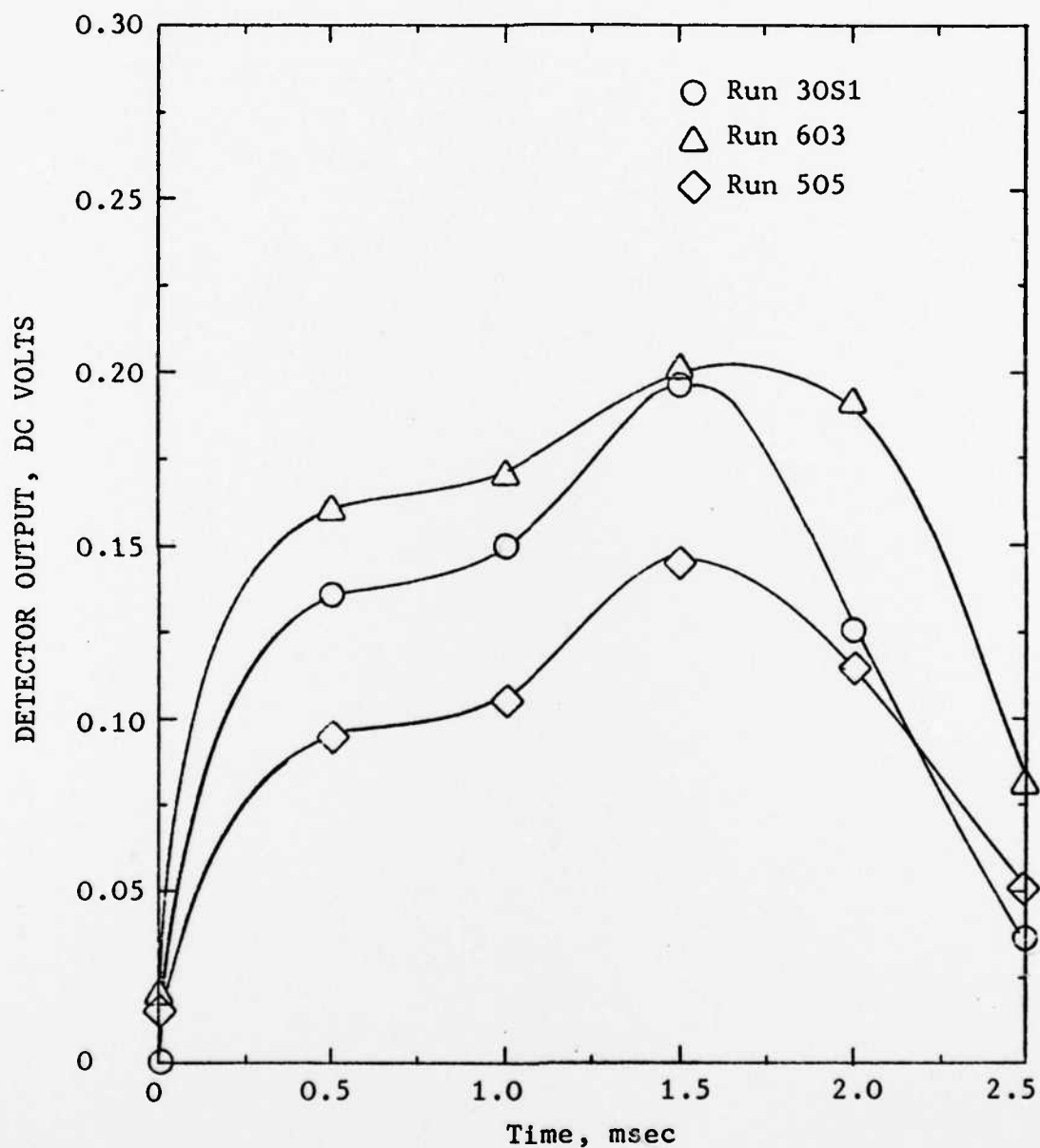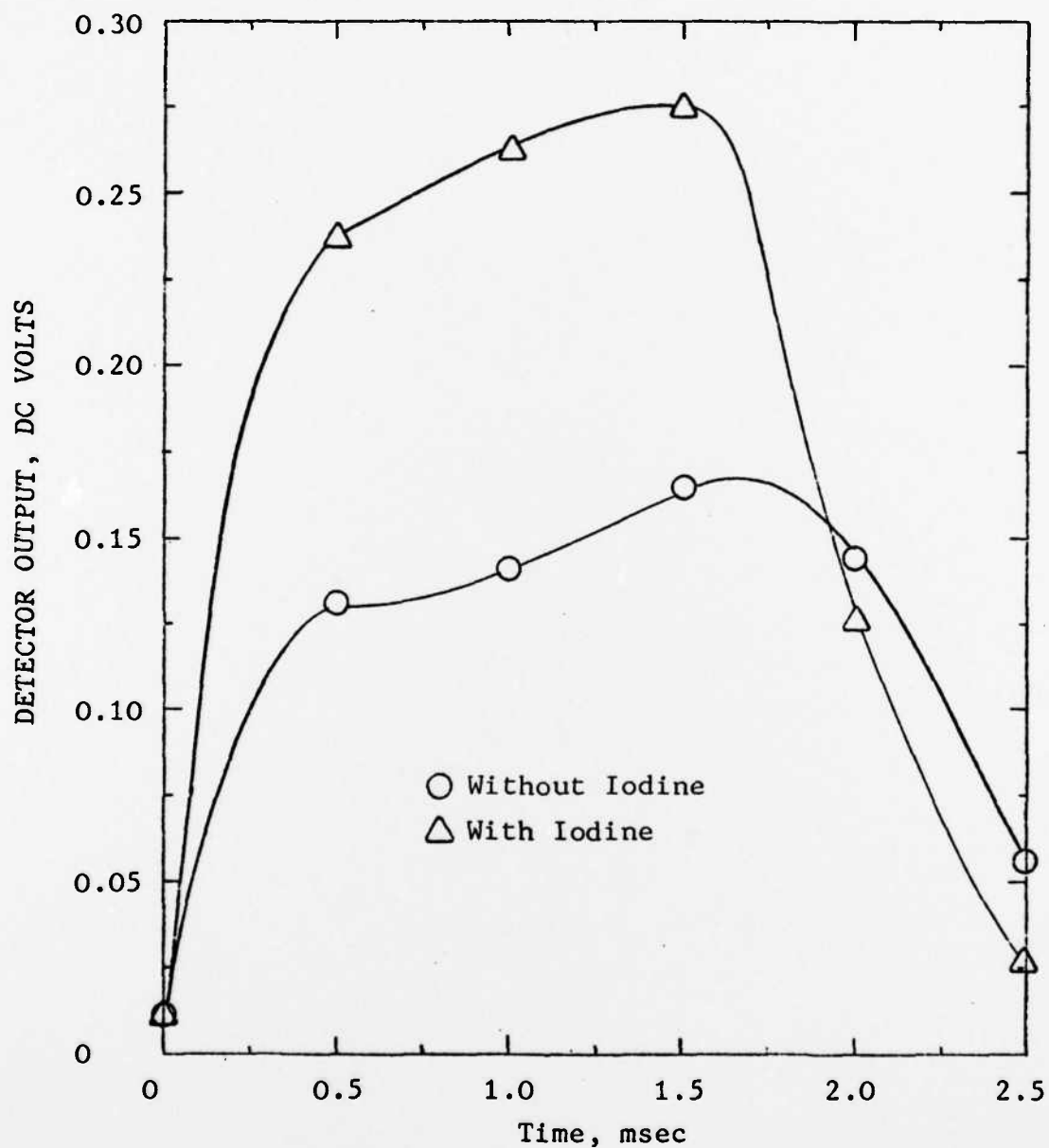## VII.   Conclusions and Recommendations

The purpose of this study was twofold. First, the
shock tube was to be reestablished in a new location and its
operational integrity verified. The second phase was to
dissociate iodine and determine if atomic iodine in an elec-
tronically excited state could be produced. Conclusions and
recommendations are offered as a result of this investigation.

Conclusions

After the shock tube was reassembled, a validity
study was conducted. As a result of this effort, the follow-
ing conclusions are made:

1.   The shock tube was established in a complete
operating configuration.

2.   It provided excellent test repeatability.

3.   Overall system reliability was acceptable.

4.   Data acquisition and reduction was straightforward.

After completion of the first phase, a preliminary
study was conducted of dissociation of iodine and infrared
emissions which were present. As a result of this effort,
the following conclusions are made:

1.   Iodine was dissociated in the shock tube.

2.   Greater intensity of emissions in the 1.1 - 5.5 μ
range were observed solely due to the addition of iodine in
the shock tube.

3.   Not enough evidence yet exists to insure that

the 1.315 μ transition can be generated with a shock wave.
However, the data presented here supports this possibility.

The purpose of this study was to establish a reliable
technique for a thorough investigation of iodine dissociation
in a shock tube. This overall objective was accomplished.

Recommendations

The feasibility of investigating the dissociation of
crystalline iodine in a shock tube has been demonstrated.
The following recommendations are offered as means to specif-
ically identify the 1.315 μ transition for iodine:

1. The optical detector system should include addi-
tional filters to limit the range of the detector to a narrow
band at 1.315 μ.

2. A rapid scan spectrometer or a fixed monochrometer
should be obtained to perform a more comprehensive study of
iodine emissions in the infrared range. This equipment could
be used to establish the population of excited atoms, the
rate at which atoms transition into the excited state, the
rate at which atoms decay into the ground state, and delay
times for these phenomena.

3. A similar study should be conducted using helium
as a test gas in that other researchers indicate that helium
may minimize quenching of atomic iodine.

As a result of the information gained from this initial
investigation of iodine dissociation, the following recom-
mendations for the shock tube facility are made:

41

1. The driven section vacuum and venting system line fittings should be replaced with high vacuum connectors in an attempt to improve the scavenging characteristics of the shock tube.

2. Several manual valves should be replaced with automatic air control valves which can be operated from the remote control panel to conserve test time.

Bibliography

1. Lee, Ja H., et al. "Ultraviolet Laser Excitation Source," Applied Optics, Volume 19, No. 19, 1 October 1980.

2. Skorobogatov, G. A. "Propagation of Photodissociation Waves," Soviet Technical Physics Letters, Volume 1, No. 5, May 1975.

3. Wright, J. Shock Tubes. New York: John Wiley and Sons, Inc., 1961.

4. Greene, E. F. and P. J. Toennies. Chemical Reactions in Shock Waves. New York: Academic Press, Inc., 1964.

5. Moore, C. E. Atomic Energy Levels. Circular of the National Bureau of Standards 467, 15 June 1949.

6. Britton, D., et al. "Shock Waves in Chemical Kinetics, the Rate of Dissociation of Iodine," Discussions of the Faraday Society, No. 17, 1954.

7. -----"Shock Waves in Chemical Kinetics: Further Studies on the Rate of Dissociation of Molecular Iodine," The Journal of Chemical Physics, Volume 25, No. 5, November 1956.

8. Liepman, H. and A. Roshko. Elements of Gas Dynamics. New York: John Wiley and Sons, Inc., 1957.

9. Gaydon, A. G. and I. R. Hurle. The Shock Tube in High Temperature Chemical Physics. New York: Rinehold Publishing Corp., 1963.

10. Burgrim, E., et al. "Efficiency of the Vibrational Deactivation and Quenching of an Electronically Excited I_2 Molecule," Opt. Spectrosc., Volume 37, No. 6, December 1974.

11. Zalesskii, V. and M. Ivanov. "Possibility of the Development of a CF_3I Glow-Discharge Laser," Soviet Journal of Quantum Electronics, Volume 5, No. 2, August 1975.

12. Chapman, A. and W. Walker. Introductory Gas Dynamics. New York: Holt, Rinehart, and Winston, Inc., 1971.

13. Jones, J. T. _Boron Ignition Limit Curve as Determined by a Shock Tube Study_. Unpublished thesis. Wright-Patterson AFB, Ohio: Air Force Institute of Technology, June 1968.

14. Pchelkin, N. R. _Initial Shock Tube Kinetic Studies of Monomethylamine_. Unpublished thesis. Wright-Patterson AFB, Ohio: Air Force Institute of Technology, December 1976.

15. Glass, I. I. and J. Hall. _Shock Tubes, Part I and II_. Toronto: University of Toronto, Institute of Aerophysics, May 1958.

APPENDIX

Experimental Data Summary

Data from the tables in this appendix were used to select the shock tube tests presented in this study and to plot Figs 14 and 15.

TABLE III

Significant Test Parameters

Run Number Day/Mo/#	Iodine	Window	P_4/P_1	P_5/P_1	M_5	T_5, K
28S2	Yes	Plexiglass	33.9	37.9	2.54	1564
30S1	No	Plexiglass	33.4	37.5	2.52	1547
505	No	Quartz	34.4	36.2	2.56	1571
603	No	Quartz	34.3	38.4	2.59	1594

TABLE IV

Detector Output for Each Test

Time, msec	Detector Output, Volts			
	Run 28S2*	30S1*	505	603
0	0.012	0	0.015	0.02
0.5	0.236	0.137	0.095	0.16
1.0	0.261	0.149	0.105	0.17
1.5	0.273	0.197	0.145	0.20
2.0	0.124	0.124	0.115	0.19
2.5	0.025	0.037	0.05	0.08

*c_f corrected data

VITA

Captain Lawrence C. Farnell was born on 20 April 1949 at Fort Benning, Georgia. He graduated from high school in Honolulu, Hawaii in 1967 and attended the University of Alabama from which he received the degree of Bachelor of Science in Aerospace Engineering in January 1972. Upon graduation, he received a commission in the USAF through the ROTC program. He was assigned to the Air Force Foreign Technology Division at Wright-Patterson AFB, Ohio in February 1972 as a Spacecraft Systems Analyst. In December 1974 he was assigned to the 390th Strategic Missile Wing, Davis-Monthan AFB, Arizona where he served as a Titan II ICBM Missile Combat Crew Commander and Director of Recurring Training. He received the degree of Master of Arts in Social Science with Emphasis in Public Administration from the University of Northern Colorado in June 1978. He entered the School of Engineering, Air Force Institute of Technology in June 1979.

                    Permanent Address: 1632 Walea Street
                                        Wahiawa, Hawaii 96786

SECURITY CLASSIFICATION OF THIS PAGE *(When Data Entered)*

REPORT DOCUMENTATION PAGE		READ INSTRUCTIONS BEFORE COMPLETING FORM
1. REPORT NUMBER AFIT/GAE/AA/80D-5	2. GOVT ACCESSION NO. AD-A094 760	3. RECIPIENT'S CATALOG NUMBER
4. TITLE *(and Subtitle)* IODINE DISSOCIATION IN A SHOCK TUBE		5. TYPE OF REPORT & PERIOD COVERED MS Thesis
		6. PERFORMING ORG. REPORT NUMBER
7. AUTHOR(s) Lawrence C. Farnell Captain, USAF		8. CONTRACT OR GRANT NUMBER(s)
9. PERFORMING ORGANIZATION NAME AND ADDRESS Air Force Institute of Technology (AFIT/EN) Wright-Patterson AFB, OH 45433		10. PROGRAM ELEMENT, PROJECT, TASK AREA & WORK UNIT NUMBERS
11. CONTROLLING OFFICE NAME AND ADDRESS Air Force Institute of Technology (AFIT/EN) Wright-Patterson AFB, OH 45433		12. REPORT DATE December 1980
		13. NUMBER OF PAGES 55
14. MONITORING AGENCY NAME & ADDRESS*(if different from Controlling Office)*		15. SECURITY CLASS. *(of this report)* UNCLASSIFIED
		15a. DECLASSIFICATION/DOWNGRADING SCHEDULE

16. DISTRIBUTION STATEMENT *(of this Report)*

Approved for public release; distribution unlimited.

17. DISTRIBUTION STATEMENT *(of the abstract entered in Block 20, if different from Report)*

18. SUPPLEMENTARY NOTES
Approved for public release IAW AFR 190-17

FREDRIC C. LYNCH, MAJOR, USAF   30 DEC 1980
Director of Public Affairs

19. KEY WORDS *(Continue on reverse side if necessary and identify by block number)*
SHOCK TUBE
IODINE LASER
DISSOCIATION
SHOCK WAVE

20. ABSTRACT *(Continue on reverse side if necessary and identify by block number)*
A two-in. (5.08 cm) I.D. circular shock tube was assembled to study the dissociation of iodine. This study was an initial investigation into the possible use of shock waves to dissociate iodine in an electronically excited state. Iodine has an emission transition in this state at a wavelength of 1.315 µ which is used in the iodine laser. Using argon as the diluent gas, tests were observed with an indium-antimonide detector to determine if

DD FORM 1473 EDITION OF 1 NOV 65 IS OBSOLETE   UNCLASSIFIED
1 JAN 73

SECURITY CLASSIFICATION OF THIS PAGE *(When Data Entered)*

DATE
ILMED